Hindawi
Journal of Nanomaterials
Volume 2017, Article ID 9701251, 13 pages
https://doi.org/10.1155/2017/9701251

Research Article

Enhancement of Fluorescence and Photostability Based on Interaction of Fluorescent Dyes with Silver Nanoparticles for Luminescent Solar Concentrators

Sara El-Molla,[1,2] A. F. Mansour,[1] and A. E. Hammad[1,3]

[1] *Physics Department, Faculty of Science, Zagazig University, Zagazig, Egypt*
[2] *Institute for Nanoelectronics, Technical University of Munich, 80333 Munich, Germany*
[3] *Basic Sciences, College of Engineering, University of Business and Technology (UBT), Jeddah, Saudi Arabia*

Correspondence should be addressed to Sara El-Molla; sara.el-molla@tum.de

Received 27 June 2017; Revised 15 August 2017; Accepted 6 September 2017; Published 15 October 2017

Academic Editor: Giuseppe Compagnini

For luminescent solar concentrators (LSCs), it is important to enhance the fluorescence quantum yield (FQY) and photostability. Our measurements have demonstrated that the addition of silver nanoparticles to dye solution causes broadening of absorption bands, so the spectral range of sunlight absorbed by LSC has increased. Silver nanoparticles (NPs) were characterized by X-ray diffraction (XRD) and UV-Vis absorption spectra. UV-Vis spectrum showed a single peak at 442 nm due to the surface plasmon resonance (SPR). The position of SPR peak exhibited a red shift after the sample was exposed to UV irradiation (unfiltered light). The optical band gap values have a reduction from 2.46 to 2.37 eV after irradiation for 960 minutes. Such reduction in optical band gap may be due to change in particle size calculated using Mie theory. The photostability of organic dyes used was improved after adding silver nanoparticles. The area under fluorescence spectra of dyes with silver NPs increased by 41–31% when compared with identical dye concentrations without silver nanoparticles as a result of interaction of the species with silver NPs.

1. Introduction

Luminescent solar concentrators (LSCs) were introduced for the first time in 1976 by Weber and Lambe [1] and then studied in detail [2, 3]. LSCs can accept both diffuse and direct sunlight and certainly it is considered that LSCs can perform better under diffuse light than under direct light, so a sunlight tracking system is unnecessary. The LSCs generally contain fluorescent particles such as organic dyes or quantum dots embedded in a transparent matrix medium such as poly(methyl methacrylate), polycarbonate, glass, or even a liquid solution. A typical fluorescent collector absorbs the incident sunlight through the front face of a luminescent plate and a fraction of the reemitted photons are trapped by total internal reflection (TIR) and directed towards a PV cell generally mounted on the edges of the collector. The luminescent solar concentrators using liquid solutions contained between transparent plates have received a little attention [4, 5]. Moreover, they represent an interesting fundamental system which can be used for a wide range of theoretical and spectroscopic studies, helping to understand the basic performance of fluorescent dye under illumination. Tummeltshammer et al. [6] simulated the efficiency of LSC which employs silver, Ag, nanoparticles to enhance the dye absorption and scatter the incoming light. It was reported that the normalized optical efficiency can be increased from 10.4% for a single dye LSC to 32.6% for a plasmonic LSC with Ag spheres immersed inside a thin dye layer. Enhancement of the efficiency was due to scattering of the particles and not due to dye absorption/reemission. As well, Holland and Hall discussed the enhanced fluorescence from molecules deposited on the surface of an optical waveguide structure. The enhancement was due to the near-field interaction between the Rhodamine B molecules and the waveguide's modal fields [7]. Meyer and Markvart showed that fluorescence spectra of an optically thick medium can be compared to a quasi-black-body radiation with a nonzero chemical potential. It was reported that photons enter into thermal equilibrium upon perfect absorption and reemission, resulting in an equal chemical potential for all photons in the system. It was shown that

photon reabsorption known also as photon recycling gradually brings the emitted photon flux into thermal equilibrium with the collector. Moreover, the key difference is that the chemical potential flux in FSCs is closer to the thermodynamical limit than the chemical potential observed for solar cells [8].

One of the major factors that affect the efficiency of a LSC module is the fluorescence quantum yield (FQY) of the luminescent species used in its design. It has been well established that the fluorescence of dye molecules can be intensified by their interaction with silver plasmons [9–13]. The enhancement of the fluorescence emission of molecules near a metal surface arises from interactions with surface plasmon resonance (SPR) in the metal particles; these interactions may also result in shorting of the excited-state lifetime leading to an improvement in the photostability of the dye [14].

When silver nanoparticles (NPs) are added to the dye solution, the dye molecules will be adsorbed on islands films of the metallic NPs. Also, when the surface plasmon resonance (SPR) of the metallic NPs coincides with the dye absorption band, it will modify the intensity of the electromagnetic field around the molecules which will increase the emitted fluorescence intensity [15]. The modification of the electromagnetic field is due to the very high field gradient near the metallic surface [16].

Mansour examined copolymer films of styrene (ST) with methyl methacrylate (MMA) of different percentage. Differential scanning calorimetry showed a single glass transition at 50/50 ST/MMA. Also, the FTIR spectra of copolymer 50/50 ST/MMA after exposure to UV radiation for 24 h were similar to those before exposure to UV radiation; this indicates that the copolymerization of styrene with MMA modifies the photodegradation behavior of polystyrene [17]. In addition, the value of the band tail of copolymer and homopolymer increased after exposure to UV radiation, while the band gap (E_g) decreased.

Chahal et al. studied the effect of ultraviolet irradiation on the optical and structural properties of PVP-Ag nanocomposite. The optical band gap values reduced from 4.90 eV in pure PVP to 4.11 eV for PVP-Ag nanocomposite prior to irradiation. This value is further reduced to 3.55 eV after UV irradiation for 180 minutes [18].

Jaleh et al. studied the effect of UV radiation on the optical properties, crystallinity, surface energy, and degradation of polystyrene (PS) and PS-TiO_2 nanocomposite. It was found that the optical band gap values reduced from 4.54 eV in pure PS to 4.45 eV for PS-TiO_2 nanocomposite prior to irradiation. This value was further reduced to 3.46 after UV irradiation for 45 h [19]. Debije and Rajkumar studied direct versus indirect illumination of a prototype luminescent solar concentrator. It was illustrated that the LSC device did improve in relative efficiency of the system under cloudy and diffuse light conditions, verifying earlier expectations [20].

In the present work, we aimed to study behavior of silver NPs before and after UV irradiation and enhance the fluorescence of selected organic dyes used in LSC by adding silver nanoparticles into the dye solutions. The photostability and energy gaps of organic dyes before and after adding silver NPs and after UV irradiation have been also investigated.

2. Experimental Procedures

The organic dyes used in this research were obtained from Radiant Dye Laser Accessories GmBH; silver NPs were obtained from Merck. The solvent used is Triton X-100 supplied by Merck. Triton X-100 is favorable because of its highly polar properties which permits dye being studied to dissolve completely in it. Plate samples of thickness ~0.02 cm and dye concentration of 10^{-4} ML^{-1} were prepared by casting method. The dye was homogeneously diffused in the polymer before casting. The samples were irradiated by a 300 W Xenon arc lamp which has a similar spectrum to the sun for 960 minutes with absorbing UV filter and without filter. Xenon arc lamps have a relatively smooth emission curve in the UV to visible spectra, with characteristic wavelengths emitted from 750 to 1000 nm. Absorption spectra for Coumarin 6, Fluorescein, and Rhodamine 6G in Triton X-100 without and with silver NPs were measured from 190 to 900 nm using UV/Visible absorption spectrometer Perkin-Elmer Lambda 4B. The spectra were recorded for the samples in the form of rectangular discs of area of 3×1 cm^2 and thickness of 0.02 cm. Fluorescence spectra were detected by a Shimadzu RF-5301 PC spectrofluorimeter (Kyoto, Japan) equipped with a 150 W Xenon lamp and using 1.0 cm quartz cells. Details of internal microstructural features are examined by transmission electron microscope (TEM).

3. Results and Discussion

3.1. Characterization of Silver Nanoparticles

3.1.1. Transmission Electron Microscope (TEM). Composites films of PVA-silver NPs were prepared and then UV-irradiated for different times. These composites films were dissolved in distilled water to record the TEM images, as shown in Figures 1(a) and 1(b). It is clearly depicted from TEM micrographs that, before UV exposure, silver NPs dispersed in PVA matrix are of concentrations with almost spherical shape and about 202–96 nm in size, as shown in Figure 1(a). After exposure to UV radiation for 960 min, silver NPs are uniformly disturbed within PVA matrix, as seen in Figure 1(b). Also, silver NPs after UV irradiation have no definite shape and particle size decreased to 89–65 nm.

3.1.2. Absorption Spectroscopy. Figures 2(a)–2(d) represent the optical absorption spectra of silver nanoparticles in Triton X-100 exposed to UV radiations (unfiltered light) for different times varying from 0 to 960 minutes. Curve (a) in this figure shows surface plasmon resonance (SPR) peak at 442 nm with the width of the absorption peak 83 nm. This deep intense absorption band is observed due to the collective excitation of all the free electrons in the surface of the metal nanoparticles. The particle size of silver NPs is calculated from half width at half-maximum (HWHF) of the optical absorption peaks using Mie theory equation [21–23] and tabulated in Table 1.

$$2R = \frac{\lambda_{\max}^2 \nu_f}{\pi c \omega}, \quad (1)$$

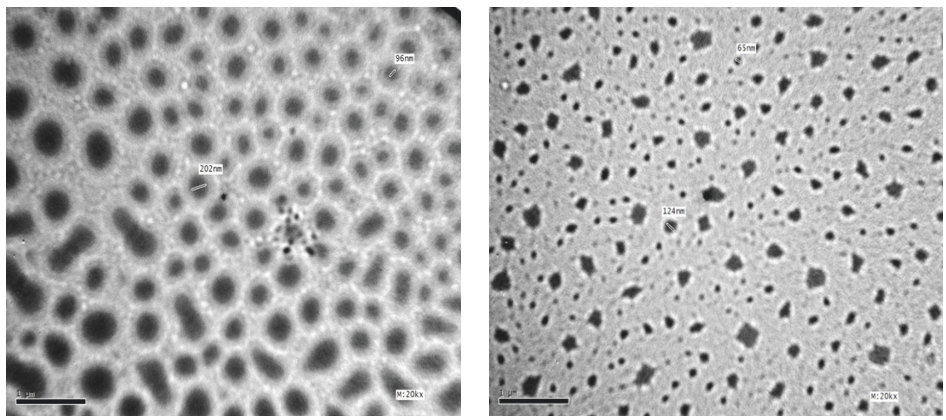

(a) (b)

Figure 1: Transmission electron microscope (TEM) with particle size of PVA/silver nanocomposites (a) before exposure to UV radiation and (b) after exposure to UV radiation for 960 minutes.

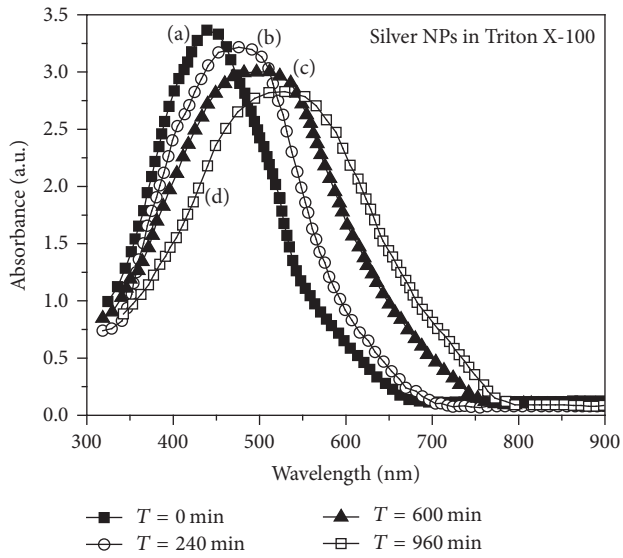

Figure 2: Absorption spectra of silver NPs in Triton X-100 before and after exposure to UV radiations (unfiltered light).

where λ_{max} is the wavelength at maximum intensity of the SPR, v_f is the velocity of the electron at Fermi levels (1.4×10^6 ms^{-1} for silver), c is the velocity of light in free space, and w is the half width at half-maximum (HWHM). It is clear that particle size decreases with increasing UV exposure time. The same behavior has been reported for polyvinylcarbazole (PVK) [24]. It was found that particle size analysis PVK with different UV irradiation times showed a size of 10.3 nm before irradiation, 8.1 nm after 1 s, and 10.5 nm after 60 s. These data proposed that photoscission rates are faster than photooxidation rates and result in shorter vinyl chains at time of 1 s. At time of 10 s, oxygen ions, for example, O^- and O_2^-, and radicals, for example, O^*, generated by UV irradiation lead to bridging oxygen between carbazole groups and result in an increase of particle size.

The absorption band is red shifted and HWHM increases from 83 to 132 nm with increase in exposure time to UV radiations due to the reduction in the particle size of silver NPs as calculated in Table 1.

3.1.3. Optical Band Gap. The optical band gaps, E_g, were calculated by the following Tauc's expression [25]:

$$(\alpha h\nu)^2 = B\left(h\nu - E_g\right), \tag{2}$$

where α is the absorption coefficient corresponding to the fundamental absorption edge, $h\nu$ is the photon energy, and B is the constant of proportionality. The values of optical band gap, E_g, can be deduced from the intercept of the linear fitted lines in the plots of $(\alpha h\nu)^2$ versus $h\nu$, as shown in Figure 3(a).

The values of optical band gap so determined are listed in Table 2. It is clear from the table that the value of E_g decreases from 2.46 to 2.37 eV after UV irradiation for 960 minutes which is in accordance with [26]. Such reduction in optical band gap may be due to change in particle size calculated using Mie theory.

Urbach's energy corresponds to the width of the tail of the localized states within the optical band gap. It is linked to the absorption coefficient in the lower energy region of fundamental edge and can be described by the relation [27]

$$\alpha(\nu) = \alpha_o \exp\left(\frac{h\nu}{E_u}\right), \tag{3}$$

where α_o is constant and E_u is the Urbach's energy. From previous equation, it is obvious that the plot of $\ln(\alpha)$ versus $h\nu$ should follow the linear behavior. Figure 3(b) presents such plots for silver NPs before and after UV radiations for different times. The determined values of Urbach's energy are listed in Table 2. It is evident from this table that E_u increases from 0.045 to 0.061 eV after irradiation for 960 minutes.

3.2. Characterization of Fluorescent Dyes in Triton X-100 with Presence of Silver NPs

3.2.1. Absorption Spectroscopy. Figures 4(a)–4(c) show the absorption spectra of Coumarin 6, Fluorescein, and Rhodamine 6G in Triton X-100, respectively, without and with

Table 1: Particle size calculated from Mie theory.

UV exposure time (min)	SPR peak (nm)	FWHM (nm)	Particle size (nm)	Uncertainty
0	442	83	4.20 3.90 3.50 4.50 3.70	±0.40
240	469	96	4.10 3.10 3.40 3.90 2.90	±0.52
600	503	119	3.40 2.80 3.15 3.60 2.70	±0.39
960	523	132	3.20 2.70 3.07 3.10 2.60	±0.26

Table 2: The values of optical band gap and Urbach's energy for silver NPs in Triton X-100 before and after exposure to UV radiation for different times.

UV exposure time (min)	Optical band gap E_g (eV)	Uncertainty	Urbach's energy E_u (eV)	Uncertainty
0	3.00 2.40 2.43 2.46 2.50	±0.25	0.053 0.050 0.045 0.043 0.060	±0.006
240	2.90 2.39 2.43 2.49 2.50	±0.21	0.059 0.055 0.047 0.049 0.062	±0.006
600	2.70 2.38 2.40 2.47 2.49	±0.13	0.061 0.060 0.054 0.050 0.063	±0.0054
960	2.55 2.38 2.37 2.40 2.47	±0.08	0.063 0.067 0.061 0.053 0.065	±0.0054

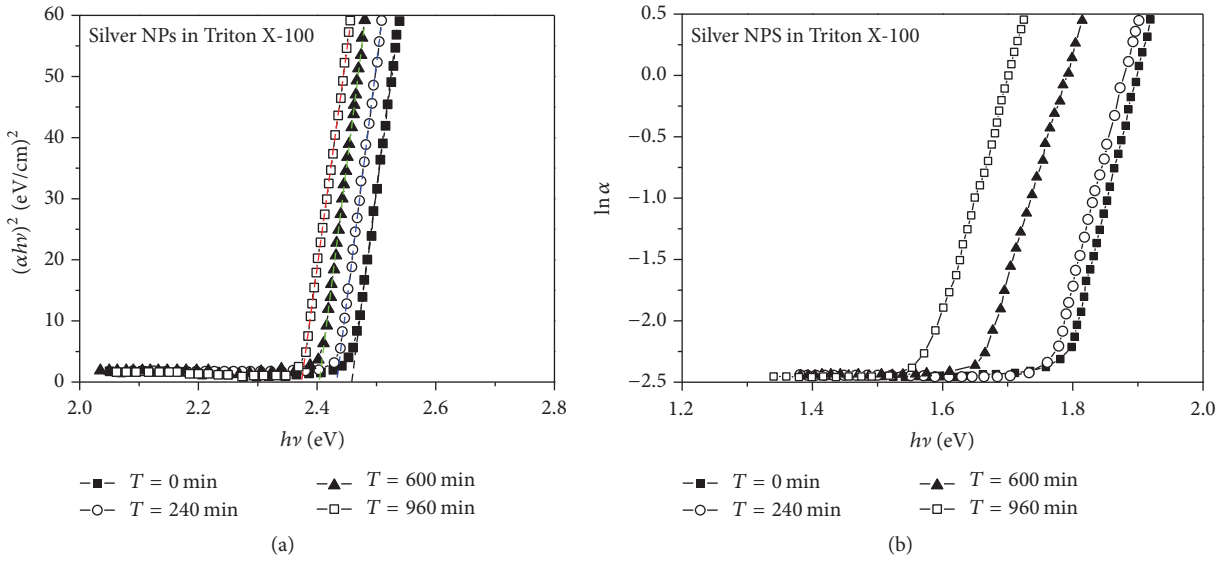

Figure 3: Plots of (a) $(\alpha h\nu)^2$ versus $h\nu$ and (b) $(\ln \alpha)$ versus $h\nu$ for silver NPs before and after exposure to UV irradiation.

silver NPs. The addition of silver NPs to dye solution causes the broadening of absorption bands, as shown in Figure 4(b), so the fluorescent species used utilizes abroad section of solar spectrum. Fluorescent dye without silver NPs exhibited peak 470 nm in the visible region. The 470 nm peak showed a broad feature with a full width at half-maximum absorbance of 49.5 nm. Furthermore, fluorescent dye with silver NPs after UV exhibited peak 475 nm in the visible region. The 475 nm peak showed a broad feature with a full width at half-maximum absorbance of 70 nm. It was found that the percentage increase in absorbed energy from fluorescent to NP/fluorescent dyes after UV is equal to 1.01. In the absorption spectrum of the dyes, we do not observe an additional peak due to silver plasmon which means that we do not have Foster energy transfer but rather a different type of interaction. The enhancement in the silver-dye system is attributed to resonance energy transfer initiated by Raman scattering. It is noted that the incident wavelength energy indicated is not the same energy that exits the sample (i.e., the fluorescence of the system). In addition, it is expected that the electric field interaction from the incident light to the nanoparticle has an effect on the enhancement as well. The overall response is best documented by Mie's theory of scattering [28].

Figure 4(c) shows the absorption spectra of dyes with silver NPs exposed to UV irradiation for 960 minutes. It is clear from this figure that the absorption peak red shifted after UV irradiation.

3.2.2. Optical Energy Gap. Figures 5(a)–5(f) show the plots of $(\alpha h\nu)^2$ versus $h\nu$ for Coumarin 6, Fluorescein, and Rhodamine 6G in Triton X-100, respectively, without and with silver NPs and also after UV irradiation for 960 minutes. Figures 6(a)–6(f) show the plots of $\ln \alpha$ versus $h\nu$ for Coumarin 6, Fluorescein, and Rhodamine 6G in Triton X-100 without and with silver NPs and also after UV irradiation for 960 minutes.

The values of optical band gap Urbach's energy are listed in Table 3. It is clear from the table that the value of E_g decreases and that of E_u increases after adding silver NPs to dye solution and also after UV irradiation for 960 minutes. Such a reduction in E_g values can be attributed to the interaction between the electric dipoles of the dye molecules and the surface plasmon of silver NPs. Also, there is a clear blue shift in the values of optical band gap after UV irradiation (without filter) for 960 minutes to dye/silver/Triton X-100. The change in E_g with UV irradiation may be attributed to quantum confinement [29].

3.3. Photostability. The stability of fluorescent dyes is one of the main factors in LSC development. To examine the stability of Coumarin 6, Fluorescein, and Rhodamine 6G in Triton X-100, the absorbance was measured before and after irradiation with 300 W Xenon arc lamp with absorbing UV filter and without filter for 960 minutes. Silver NPs added to the above samples and measurements are repeated. Figures 7(a)–7(f) show improving stability of organic dyes used after addition of silver NPs. This highlights the importance of silver NPs especially with Rhodamine 6G which experiences photobleaching after exposure for 35 min without silver.

The stability of the organic dyes may be due to the interaction with surface plasmon resonance (SPR) in metal particles; there is also interaction result in shorting of the excited-state lifetime thus improving the photostability of the dye [14]. Audino and Geddes studied the enhanced photostability of fluorophores in the presence of antioxidants and plasmon supporting nanoparticles [30]. It was reported that enhanced photostability was possible due to a coupling in both the fluorophore's ground and excited state, with the emission of the coupled quanta originating from the nanoparticle itself. Also, it was reported that micrometer-sized, bovine serum albumin (BSA) or polyethylene glycol (PEG) coated PDMS wells can

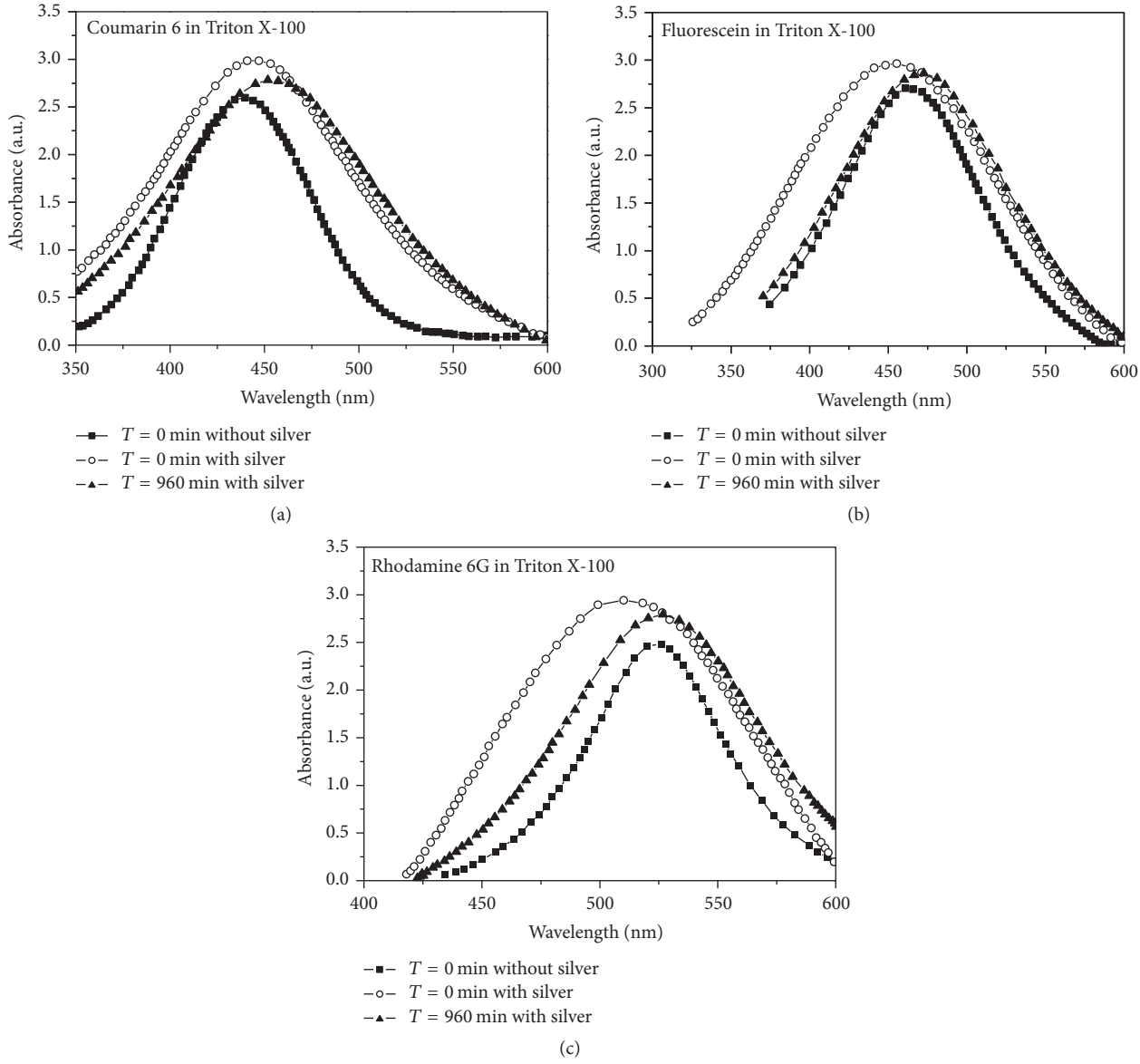

Figure 4: Absorption spectra of (a) Coumarin 6, (b) Fluorescein, and (c) Rhodamine 6G in Triton X-100 with/without silver before and after UV irradiation.

Table 3: The values of optical band gap and Urbach's energy for Coumarin 6, Fluorescein, and Rhodamine 6G in Triton X-100 with and without silver NPs before and after exposure to UV irradiation.

Dyes	Before adding silver	E_g	E_u	After adding silver	E_g	E_u
Coumarin 6	$T = 0$	2.56	0.066	$T = 0$	2.47	0.073
	$T = 960$ min with filter	2.51	0.069	$T = 960$ min with filter	2.47	0.075
	$T = 960$ min without filter	2.49	0.071	$T = 960$ min without filter	2.43	0.077
Fluorescein	$T = 0$	2.30	0.039	$T = 0$	2.27	0.051
	$T = 960$ min with filter	2.29	0.041	$T = 960$ min with filter	2.27	0.052
	$T = 960$ min without filter	2.28	0.042	$T = 960$ min without filter	2.26	0.054
Rhodamine 6G	$T = 0$	2.19	0.044	$T = 0$	2.16	0.062
	$T = 40$ min with filter	2.18	0.045	$T = 960$ min with filter	2.16	0064
	$T = 35$ min without filter	2.17	0.046	$T = 960$ min without filter	2.15	0.067

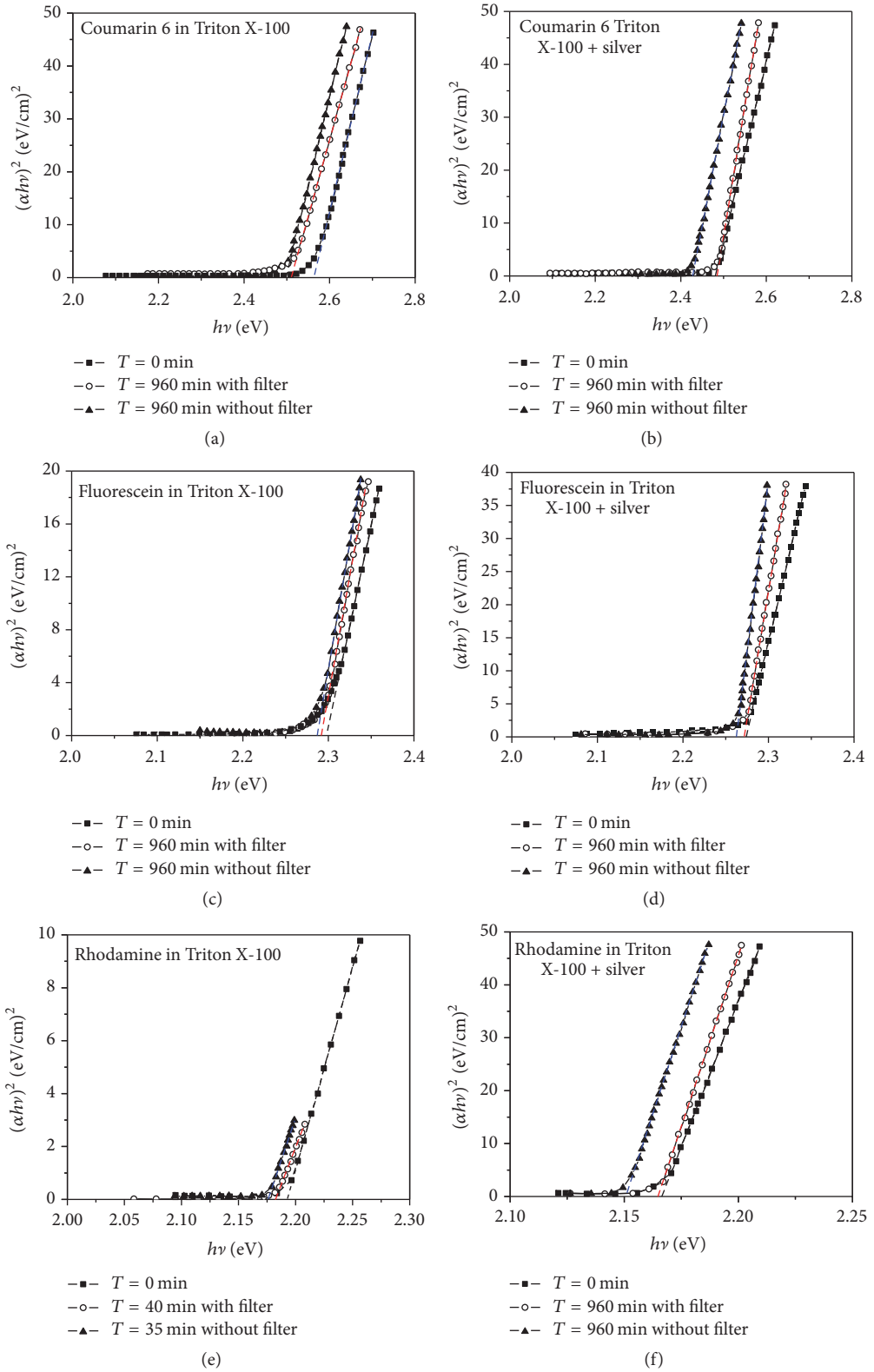

FIGURE 5: Plots of $(\alpha h\nu)^2$ versus $h\nu$ for Coumarin 6, Fluorescein, and Rhodamine 6G in Triton X-100 without and with silver NPs before and after exposure to UV irradiation with filter and without filter.

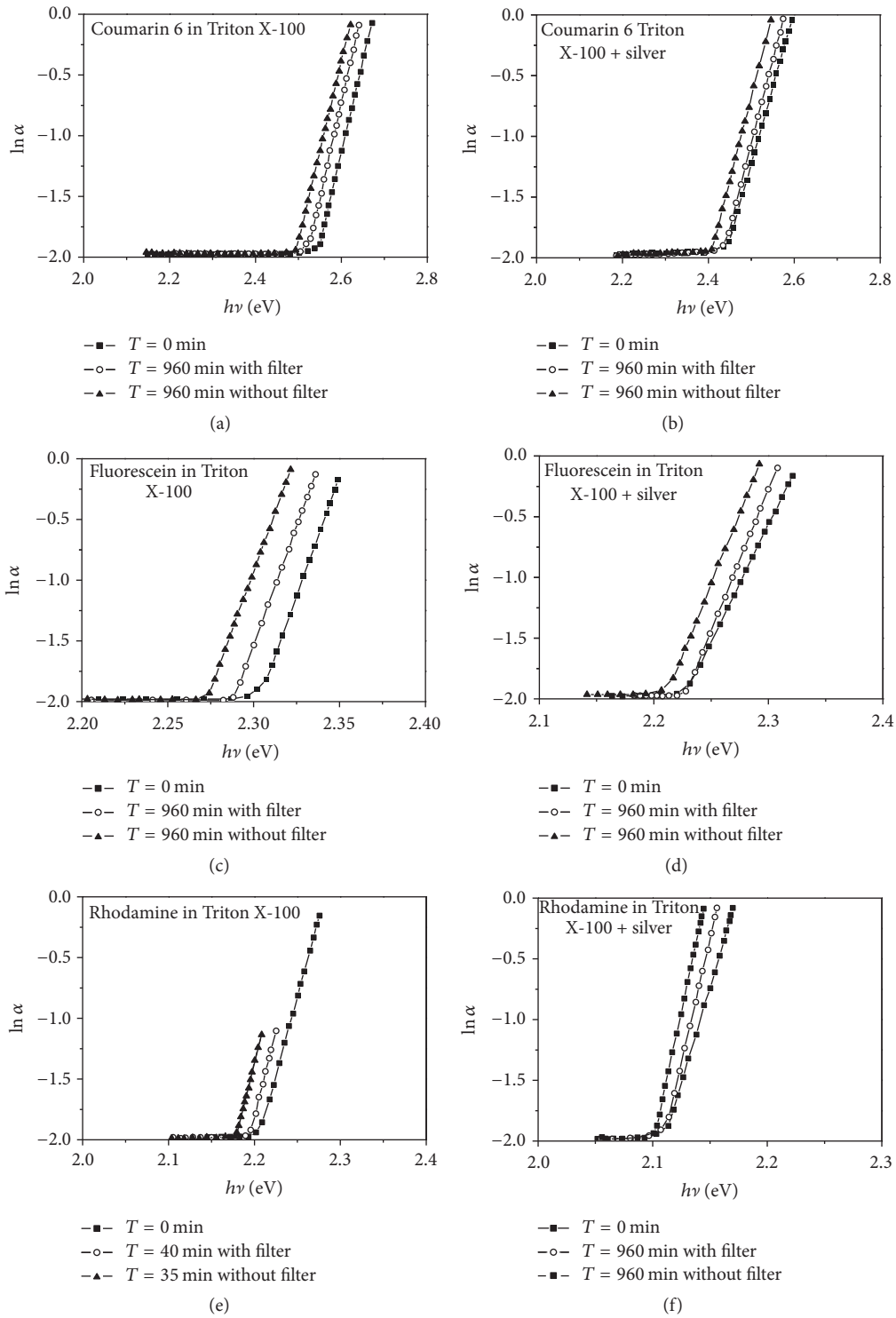

Figure 6: Plots of $\ln \alpha$ versus $h\nu$ for Coumarin 6, Fluorescein, and Rhodamine 6G in Triton X-100 without and with silver NPs before and after exposure to UV irradiation with filter and without filter.

Table 4: The kinetics of photodegradation (K) and half-life time ($t_{1/2}$) of dyes/Triton X-100 and dyes/silver NPs/Triton X-100.

Dyes	Conditions	Without filter		With filter	
		K (min^{-1})	$t_{1/2}$ (min)	K (min^{-1})	$t_{1/2}$ (min)
Coumarin 6	Before adding silver	8.37×10^{-5}	8278	5.33×10^{-5}	12984
	After adding silver	3.49×10^{-5}	19847	1.04×10^{-6}	665694
Fluorescein	Before adding silver	9.80×10^{-5}	7062	4.85×10^{-6}	14270
	After adding silver	5.22×10^{-5}	13255	1.24×10^{-6}	554690
Rhodamine 6G	Before adding silver	4.4×10^{-2}	15.74	3.53×10^{-3}	19.59
	After adding silver	4.89×10^{-5}	14143	1.04×10^{-6}	653773

Table 5: The area under fluorescence curves for Coumarin 6, Fluorescein, and Rhodamine 6G in Triton X-100 without and with silver and with silver after UV irradiation for 960 minutes.

Dyes	Conditions	Absorbance wavelength (nm)	Emission wavelength (nm)	Stoke shift ($\Delta\lambda$) (nm)	Area under fluorescence curve
Coumarin 6	Without silver	440	538	98	486.60
	With silver before exposure	440	540	100	686.65
	With silver after exposure	455	562	107	585.68
Fluorescein	Without silver	461	542	81	614.33
	With silver before exposure	454	542	88	806.77
	With silver after exposure	472	562	90	684.93
Rhodamine 6G	Without silver	525	557	32	639.58
	With silver before exposure	510	557	47	874.26
	With silver after exposure	526	583	57	738.54

enhance the photostability of one or a few R6G molecules. Many fluorescent dyes, including R6G, undergo photobleaching via formation of radical ions, and thus, reactions that can effectively help such radical states return to the fluorophore's electronic ground states will lead to an enhancement in the photostability of the fluorescent molecules [31].

Rate constants of photodegradation of dyes are estimated according to [32]

$$K = \frac{2.3}{t} \log \frac{A_o}{A}, \quad (4)$$

where A_o and A are the absorption before and after UV irradiation, t is the time of exposure in minutes, and K is the rate constant. The kinetics of photodegradation (K) and half-life time ($t_{1/2}$) of dyes/Triton X-100 and dyes/silver NPs/Triton X-100 are listed in Table 4. Degradation means that the dye characteristic gets lost. This can be done by decomposition of the dye molecule (this means cracking the dye molecule in the way that you get smaller molecules) or changing the dye molecule by oxidation, reduction, agglutination, or other process, so that the dye characteristic gets lost (not necessarily cracking the dye molecule). Decomposition means that you will decompose the dye molecule (dividing it in parts). From results, it is clear that $t_{1/2}$ values of three fluorescent dyes after adding silver NPs are extremely increased, especially for Rhodamine 6G. Also, rate of photodegradation, K, of the examined dyes with/without filter after adding Ag NPs decreased.

3.4. Enhancing the Fluorescence of Fluorescent Dyes. Figure 8 shows the fluorescence spectra of Coumarin 6, Fluorescein, and Rhodamine 6G in Triton X-100 without and with silver NPs. From these figures, the addition of silver NPs to dye solution causes the broadening of fluorescence curves. The area under fluorescence spectra is calculated and listed in Table 5. It is clear from the table that the area increased by 41, 31, and 36% for Coumarin 6, Fluorescein, and Rhodamine 6G dyes, respectively, in Triton X-100 with silver NPs when compared with identical dye concentration without silver NPs. Also, the fluorescence spectra of fluorescent dyes with silver NPs after exposure to Xenon arc lamp 300 W without UV filter for 960 minutes decreased by 15%. This is attributed to the fact that self-absorption is increased and that leads the light that is absorbed to refluoresce in an arbitrary direction, most of which will again be trapped within the sample, and thus there will be a number of generations of fluorescence: the first one is the fluorescence resulting from the initial absorption of light; the second one is the fluorescence resulting from the self-absorption of the first one; the third one is the

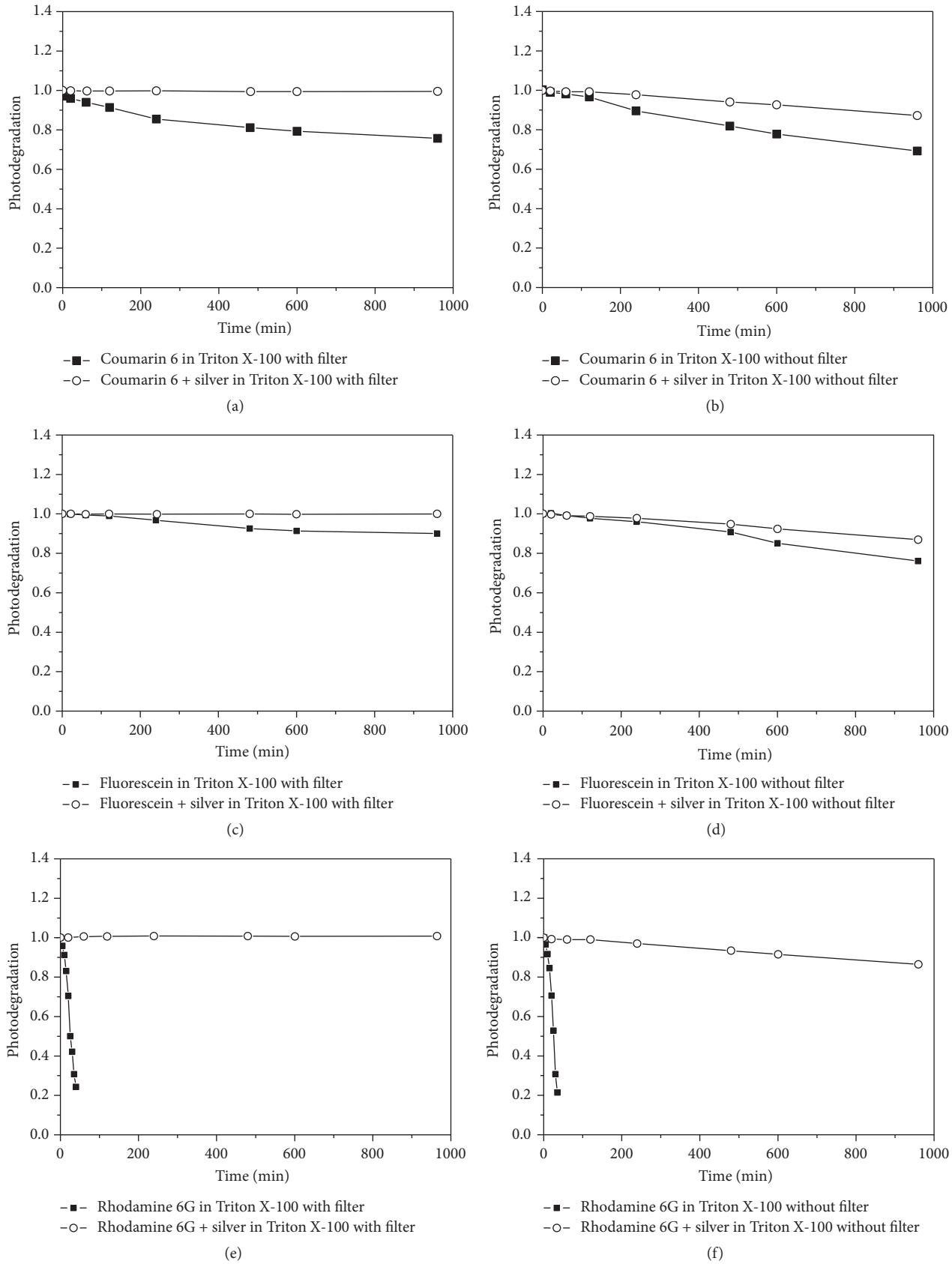

Figure 7: The photodegradation of Coumarin 6, Fluorescein, and Rhodamine 6G in Triton X-100 with and without filter before and after adding silver NPs.

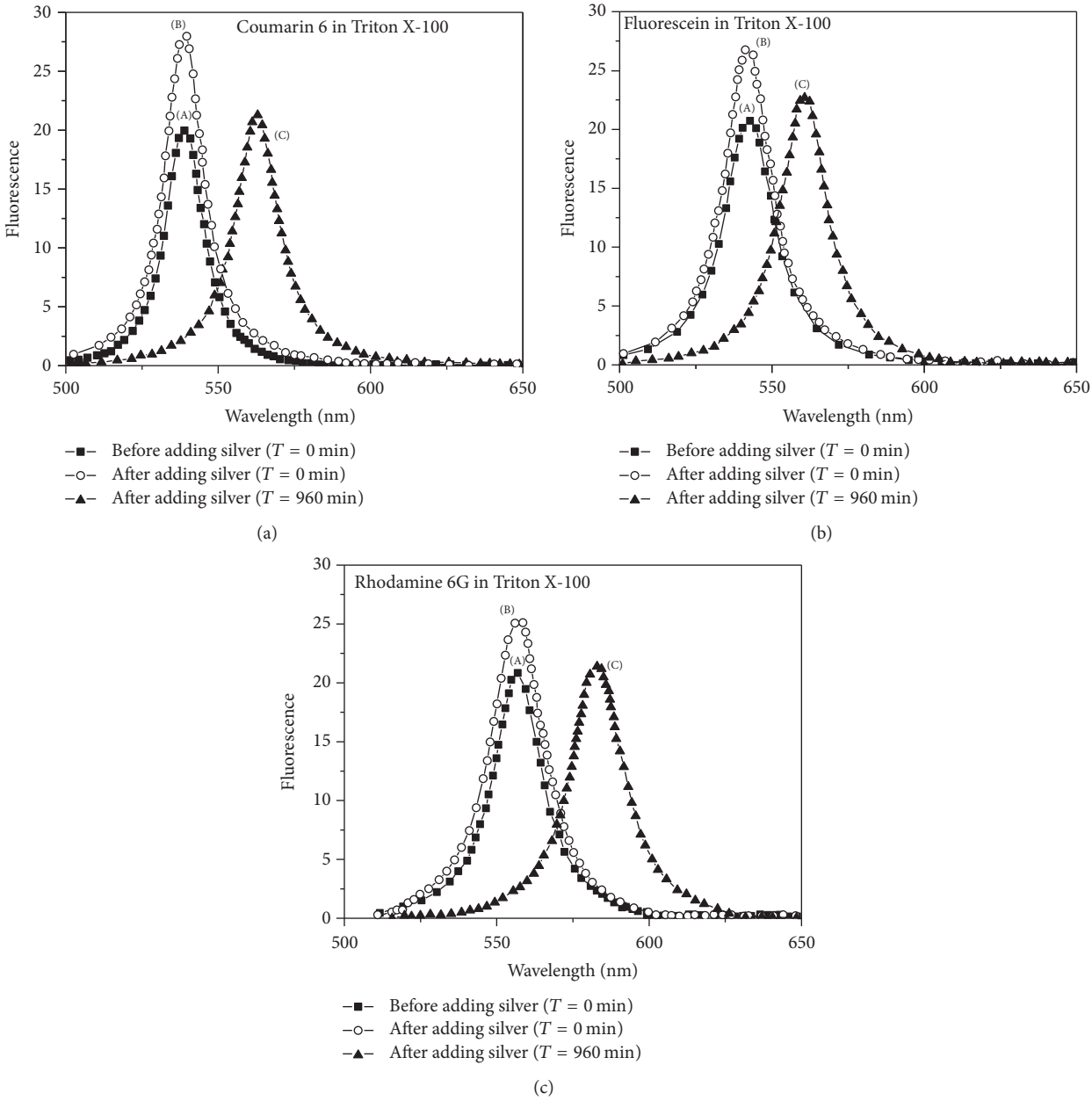

Figure 8: Fluorescence spectra of Coumarin 6, Fluorescein, and Rhodamine 6G in Triton X-100 (A) without silver, (B) with silver, and (C) with silver after UV irradiation.

fluorescence resulting from the self-absorption of the second one; and so forth, and so each generation is progressively red-shifted with respect to the preceding generation [33].

4. Conclusion

The challenges in LSC development have been highlighted. One promising concept is the addition of silver nanoparticles (NPs). The results are summarized as follows:

(1) Silver NPs in Triton X-100 were analyzed by different characterizing methods and it is confirmed that the absorption band exhibited a red shift and broadening after UV irradiation for 960 minutes.

(2) The optical energy gap (E_g) decreased and Urbach's energy (E_u) increased after irradiation for silver NPs in liquid and in solid matrix.

(3) The measurements of FQY of Coumarin 6 and Fluorescein at different concentrations reveal the dependence of FQY on concentrations.

(4) The addition of silver (NPs) to dye solution has been investigated as a means of enhancing the fluorescence of our selected dyes. The increase in fluorescence highlights the importance of silver NPs.

(5) The photostability of our selected organic dyes in liquid and solid matrix was enhanced by the addition

of silver NPs especially with Rhodamine 6G in liquid in which the photostability extremely increased.

Disclosure

Some part of this study is sequentially presented at Solar-TR-2: Solar Electricity Conference and Exhibition Programme, Turkey, 2013.

Conflicts of Interest

The authors declare that they have no conflicts of interest.

Acknowledgments

This work was supported by the German Research Foundation (DFG) and the Technical University of Munich within the Open Access Publishing Funding Programme. Also, the authors would like gratefully to thank Dr. Mohammed Gabr for his cooperation and support.

References

[1] W. H. Weber and J. Lambe, "Luminescent greenhouse collector for solar radiation," *Applied Optics*, vol. 15, no. 10, pp. 2299-2300, 1976.

[2] A. Goetzberger and W. Greube, "Solar energy conversion with fluorescent collectors," *Applied Physics*, vol. 14, no. 2, pp. 123–139, 1977.

[3] M. G. Debije and P. P. C. Verbunt, "Thirty years of luminescent solar concentrator research: solar energy for the built environment," *Advanced Energy Materials*, vol. 2, no. 1, pp. 12–35, 2012.

[4] A. A. Earp, G. B. Smith, P. D. Swift, and J. Franklin, "Maximising the light output of a Luminescent Solar Concentrator," *Solar Energy*, vol. 76, no. 6, pp. 655–667, 2004.

[5] S. T. Baily, G. E. Lokey, M. S. Hanes et al., "Optimized excitation energy transfer in a three-dye luminescent solar concentrator," *Solar Energy Materials and Solar Cells*, vol. 91, no. 1, pp. 67–75, 2007.

[6] C. Tummeltshammer, M. S. Brown, A. Taylor, A. J. Kenyon, and I. Papakonstantinou, "Efficiency and loss mechanisms of plasmonic luminescent solar concentrators," *Optics Express*, vol. 21, no. 105, pp. A735–A749, 2013.

[7] W. R. Holland and D. G. Hall, "Waveguide mode enhancement of molecular fluorescence," *Optics Letters*, vol. 10, no. 8, pp. 414–416, 1985.

[8] T. J. Meyer and T. Markvart, "The chemical potential of light in fluorescent solar collectors," *Journal of Applied Physics*, vol. 105, no. 6, p. 063110, 2009.

[9] R. Reisfeld, "Invited paper," *Optical Materials*, vol. 32, article 850, 2010.

[10] R. Reisfeld, V. Levchenko, and T. Saraidarov, "Interaction of luminescent dyes with noble metal nanoparticles in organic–inorganic glasses for future luminescent materials," *Polymers for Advanced Technologies*, vol. 22, pp. 64–66, 2011.

[11] V. Levchenko, M. Grouchko, S. Magdassi, T. Saraidarov, and R. Reisfeld, "Enhancement of luminescence of Rhodamine B by gold nanoparticles in thin films on glass for active optical materials applications," *Optical Materials*, vol. 34, no. 2, pp. 360–364, 2011.

[12] T. Saraidarov, V. Levchenko, A. Grabowska, P. Borowicz, and R. Reisfeld, "Non-self-absorbing materials for Luminescent Solar Concentrators (LSC)," *Chemical Physics Letters*, vol. 492, no. 1-3, pp. 60–62, 2010.

[13] O. D. Bekasova, "Optical properties of silver nanoparticles in R-phycoerythrin nanochannels in aqueous solutions and films," *Inorganic Materials*, vol. 46, no. 11, pp. 1201–1205, 2010.

[14] O. G. Tovmachenko, C. Graf, D. J. van den Heuvel, and A. van Blaaderen, "Fluorescence enhancement by metal-core/silica-shell nanoparticles," *Advanced Materials*, vol. 18, no. 1, pp. 91–95, 2006.

[15] M. A. Noginov, G. Zhu, M. Bahoura et al., "Enhancement of spontaneous and stimulated emission of a rhodamine 6G dye by an Ag aggregate," *Physical Review B*, vol. 74, pp. 184–203, 2006.

[16] M. A. Noginov, G. Zhu, C. Davison et al., "Effect of Ag aggregate on spectroscopic properties of Eu: Y 2 O 3 nanoparticles," *Journal of Modern Optics*, vol. 52, no. 16, pp. 2331–2341, 2005.

[17] A. F. Mansour, "Photostability and optical parameters of copolymer styrene/MMA as a matrix for the dyes used in fluorescent solar collectors," *Polymer Testing*, vol. 23, no. 3, pp. 247–252, 2004.

[18] R. Chahal, S. Mahendia, A. K. Tomar, and S. Kumar, "Effect of ultraviolet irradiation on the optical and structural characteristics of in-situ prepared PVP-Ag nanocomposites," *Digest Journal of Nanomaterials and Biostructures*, vol. 6, no. 1, pp. 301–308, 2011.

[19] B. Jaleh, M. Shayegani Madad, M. Farshchi Tabrizi, S. Habibi, R. Golbedaghi, and M. R. Keymanesh, "UV-degradation effect on optical and surface properties of polystyrene-TiO_2 nanocomposite film," *Journal of the Iranian Chemical Society*, vol. 8, no. 1, pp. S161–S168, 2011.

[20] M. G. Debije and V. A. Rajkumar, "Direct versus indirect illumination of a prototype luminescent solar concentrator," *Solar Energy*, vol. 122, pp. 334–340, 2015.

[21] A. I. Kryukov, A. L. Stroyuk, N. N. Zin'chuk, A. V. Korzhak, and S. Y. Kuchmii, "Optical and catalytic properties of Ag2S nanoparticles," *Journal of Molecular Catalysis A: Chemical*, vol. 221, no. 1-2, pp. 209–221, 2004.

[22] D. Manikandan, S. Mohan, and K. G. M. Nair, "Absorption and luminescence of silver nanocomposite soda-lime glass formed by Ag^+–Na^+ ion-exchange," *Materials Research Bulletin*, vol. 38, no. 9, pp. 1545–1550, 2003.

[23] A. Pragatheeswaran, T. Abdul Kareem, and A. Anu Kaliani, "Effect of plasma exposure on silver nanoparticles embedded in polyvinyl alcohol," *Journal of Physics: Conference Series*, vol. 208, Article ID 012109, 2010.

[24] L. Qian, D. Bera, and P. H. Holloway, "Effects of ultraviolet light irradiation on poly(vinlycarbazole)," *Applied Physics Letters*, vol. 92, no. 5, p. 053303, 2008.

[25] J. Tauc, R. Grigorovic, and A. Vancu, "Optical properties and electronic structure of amorphous germanium," *Phys Status Solidi B*, vol. 15, no. 2, pp. 627–637, 1966.

[26] R. Chahal, S. Mahendia, and A. K. Tomar, "Shymkumar," *Digest Journal of Nanomaterials and Biostructures*, vol. 6, article 299, 2011.

[27] T. Datta, J. A. Woollam, and W. Notohamiprodjo, "Optical-absorption edge and disorder effects in hydrogenated amorphous diamondlike carbon films," *Physical Review B*, vol. 40, no. 9, pp. 5956–5960, 1989.

[28] A. C. Booker, *Master of Science in Electrical and Computer Engineering [Master, thesis]*, 2006.

[29] S. M. Reda, "Synthesis and optical properties of CdS quantum dots embedded in silica matrix thin films and their applications as luminescent solar concentrators," *Acta Materialia*, vol. 56, no. 2, pp. 259–264, 2008.

[30] J. L. Audino and C. D. Geddes, "Enhanced photostability of fluorophores in the presence of antioxidants and plasmon supporting nanoparticles," *Biophysical Journal*, vol. 104, no. 2, 349a pages, 2013.

[31] L. Guo and F. Gai, "Simple method to enhance the photostability of the fluorescence reporter R6G for prolonged single-molecule studies," *The Journal of Physical Chemistry*, vol. 117, no. 29, pp. 6164–6170, 2013.

[32] I. Grabchev and V. Bojinov, "Synthesis and characterization of fluorescent polyacrylonitrile copolymers with 1,8-naphthalimide side chains," *Polymer Degradation and Stability*, vol. 70, no. 2, pp. 147–153, 2000.

[33] J. S. Batchelder, A. H. Zewai, and T. Cole, "Luminescent solar concentrators. 1: Theory of operation and techniques for performance evaluation," *Applied Optics*, vol. 18, no. 18, pp. 3090–3110, 1979.